Numerical approximation and convergence to steady state solutions of a model for the dynamics of the sexual phase of *Monogonont rotifera*

Luis M. Abia[a], Óscar Angulo[a,*], Juan Carlos López-Marcos[a]

[a] *Universidad de Valladolid, Departamento de Matemática Aplicada e IMUVA, Facultad de Ciencias, Valladolid, SPAIN*

Abstract

We consider the numerical approximation of the asymptotic behavior of an age-structured compartmental population model for the dynamics of the sexual phase of *Monogonont rotifera*. To cope with the difficulties of the infinite lifespan in long-time simulations, the main approach introduces a second order numerical discretization of a reformulation of the model problem in terms of a new computational size variable that evolves with age. The main contribution is to establish second order of convergence of the steady-state solutions of the discrete equations to the theoretical steady states of the continuous age-structured population model. Moreover, we report numerical evidence of a threshold for the male-female encounter rate parameter in the model after which the steady solution becomes unstable and a stable limit cycle appears in the dynamics. Finally, we confirm the effectiveness of the numerical technique we propose, when considering long-time integration of age-structured population models with infinite lifespan.

Keywords: age-structure population model, unbounded age, continuous-discrete dynamics, asymptotic behavior, Monogonont rotifera, numerical methods
2010 MSC: 92D25, 65M25, 65M12

*Corresponding author at: Departamento de Matemática Aplicada. Facultad de Ciencias. Universidad de Valladolid. Paseo de Belén, 7 - Campus Miguel Delibes, 47011 Valladolid, Spain. Phone: +34 983 423000 (Ext: 6646)

Email addresses: lmabia@uva.es (Luis M. Abia), oscar.angulo@uva.es (Óscar Angulo), lopezmar@uva.es (Juan Carlos López-Marcos)

1. Introduction

Population dynamics are described using various models. In particular, the variables that drive the modelling might be continuous, but the events in the population could occur at certain discrete values. Such a combination of discrete and continuous dynamics is a challenge. For instance, continuous models might include features that relate its behavior to discrete models. As a first example, discrete events in a compartmental model modify the balance equations for the individuals of the different subpopulations in the model. This is the case, for example, in particular differential-difference models [3], or in general structured epidemiological models [14]. As another example, the source term of certain population models may be impulsive to represent the encounter of two kinds of individuals; this event could only last for a short period of time and dissapear suddenly [9]. Also, discrete delays in a model may introduce different discrete artifacts in the evolution of the population [12, 4]. Most of these models cannot be solved analytically and the use of numerical techniques to approach these dynamics is essential. However, the study of discrete and continuous dynamics is quite different and it is worth showing how the dynamics of the numerical technique that approximates the solution of a model also approaches the dynamics of such model.

In this paper, as an illustration of this situation, we are going to revisit a model that describes the dynamics of a population of *Monogonont rotifera*, firstly introduced and analyzed by Calsina *et al.* [9, 11]. The study of the dynamics of this kind of microorganisms is worthwhile because of its intrinsic biological value as a model in evolutionary biology, namely its uncommon reproduction that mixes sexual and asexual phases. Moreover, as reported recently in [17], both marine and freshwater rotifera have a main role in the degradation of microplastics and their transformation into nanoplastics. Microplastics and nanoplastics are the last two stages of plastic debris before degradation to molecules during the global plastic-carbon cycle. And since nanoplastics are small enough to be in every biological trophic chain, regardless of the control systems of organisms, they represent a serious ecological problem.

The model describes the dynamics of the sexual phase of *Monogonont rotifera* by means of a compartmental model that divides the population

into three classes [9]: virgin mictic females, $\tilde{v}(\alpha,\tau)$, which are responsible for sexual reproduction because they produce the haploid males; mated mictic females, $h_m(\alpha,\tau)$, which are devoted to the asexual reproduction and produce the resting eggs; and haploid males, $\tilde{h}(\alpha,\tau)$. All of these population densities depend on both the age α and the time τ. The total population of each subclass is, respectively, $\tilde{V}(\tau)=\int_0^\infty \tilde{v}(\alpha,\tau)\,d\alpha$, $\int_0^\infty h_m(\alpha,\tau)\,d\alpha$, and $\tilde{H}(\tau)=\int_0^\infty \tilde{h}(\alpha,\tau)\,d\alpha$. These population densities fulfill the following system of integro-partial differential equations

$$\left\{\begin{array}{rcl} \tilde{v}_\tau(\alpha,\tau)+\tilde{v}_\alpha(\alpha,\tau)+\tilde{\mu}\,\tilde{v}(\alpha,\tau) &=& -\tilde{E}\,\tilde{H}(\tau)\,\tilde{v}(\alpha,\tau)\,\chi_{[0,\tilde{T}]}(\alpha),\\ (h_m)_\tau(\alpha,\tau)+(h_m)_\alpha(\alpha,\tau)+\tilde{\mu}\,h_m(\alpha,\tau) &=& \tilde{E}\,\tilde{H}(\tau)\,\tilde{v}(\alpha,\tau)\,\chi_{[0,\tilde{T}]}(\alpha),\\ \tilde{h}_\tau(\alpha,\tau)+\tilde{h}_\alpha(\alpha,\tau)+\tilde{\delta}\,\tilde{h}(\alpha,\tau) &=& 0, \end{array}\right. \tag{1.1}$$

$\alpha\geq 0$, $\tau\geq 0$, which are completed with boundary conditions

$$\tilde{v}(0,\tau)=B,\quad h_m(0,\tau)=0,\quad \tilde{h}(0,\tau)=b\int_M^\infty \tilde{v}(\alpha,\tau)\,d\alpha,\quad \tau\geq 0, \tag{1.2}$$

and an initial data

$$\tilde{v}(\alpha,\tau)=\tilde{v}^0(\alpha),\quad h_m(\alpha,\tau)=h_m^0(\alpha),\quad \tilde{h}(\alpha,\tau)=\tilde{h}^0(\alpha),\quad \alpha\geq 0, \tag{1.3}$$

where $\tilde{\delta}$ and $\tilde{\mu}$ are the mortality rates for males and females, respectively; $\tilde{E}$ is the male-female encounter rate; B is the recruitment rate of mictic females; b is the fertility of male-producing mictic females; M is the age at maturity for females; and, $\tilde{T}$ is the threshold age of fertilization ($\tilde{T}\leq M$). The source terms include the discrete event in the problem, and gives an account of the encounter among virgin mictic females and haploid males' populations. Here $\chi_{[0,\tilde{T}]}(\alpha)$ represents the characteristic function of the interval $[0,\tilde{T}]$, because the event does not occur beyond the threshold age of fertilization of virgin mictic females. We should pay attention to the discontinuity at the age $\alpha=\tilde{T}$ of the source term in (1.1) that, suddenly, changes the evolution of the populations. Following [11], the model (1.1)-(1.3) is simplified because the density of mated mictic females can be obtained once we know the other two densities. Moreover, after an appropriate change of variables

$$\begin{array}{cc} \alpha=M\,a, & \tau=M\,t,\\ \tilde{v}(\alpha,\tau)=B\,v(a,t), & \tilde{h}(\alpha,\tau)=B\,b\,M\,h(a,t), \end{array}$$

and the following notation for new non-dimensional parameters, $\mu=\tilde{\mu}\,M$, $\delta=\tilde{\delta}\,M$, $E=\tilde{E}\,B\,b\,M^3$, and $A=\tilde{T}/M$, we arrive at the system of equations

to be satisfied by the new population densities for the virgin mictic females and haploid males, that become

$$\begin{cases} v_t(a,t) + v_a(a,t) + \mu\, v(a,t) &= -E\, H(t)\, v(a,t)\, \chi_{[0,A]}(a),\ a \geq 0,\ t \geq 0, \\ h_t(a,t) + h_a(a,t) + \delta\, h(a,t) &= 0,\ a \geq 0, \quad t \geq 0, \end{cases} \tag{1.4}$$

with boundary conditions

$$v(0,t) = 1, \quad h(0,t) = \int_1^\infty v(a,t)\, da, \quad t \geq 0, \tag{1.5}$$

and initial data

$$v(a,0) = v^0(a), \quad h(a,0) = h^0(a), \quad a \geq 0. \tag{1.6}$$

The new variables a and t represent again age and time (scaled in terms of maturity). The age structures the individuals in the population, and age at maturity is 1. We denote the total number of haploid males and virgin females as

$$H(t) = \int_0^\infty h(a,t)\, da, \quad V(t) = \int_0^\infty v(a,t)\, da. \tag{1.7}$$

The existence and uniqueness of solutions for nonlinear age-dependent population models as (1.4)-(1.7) are well established when either classical analysis or nonlinear semigroups theory is used [16, 10, 15, 13]. Also, the basic linearization principle for the study of the stability of equilibria in these models is developed.

A theoretical study of the model shows the existence of unique stationary population densities which are stable if the male-female encounter rate parameter E remains below a critical value. Also, a stable limit cycle appears in the dynamics once the stability of the stationary solutions is lost [11]. In this work, a linear approach to this limit cycle is proposed.

Models like (1.4)-(1.6) cannot be solved analytically and, therefore, a numerical method to approximate its solution is needed. Moreover, the approximation of the asymptotic stationary structures of the dynamics in models like these requires long-time integrations with the numerical schemes. Different authors have studied the numerical integration of age-structured models during the last four decades [1] (and the references there in) In the case of the asymptotic study of the model, an infinite setting for the age domain is required; a fact that none of the proposed methods contribute to. Recently,

new methods that deal with this issue have been studied [2], and we will use them to give a straight approximation to the asymptotic behavior of the model (1.4)-(1.6).

In this paper, we can afford an extension of the convergence analysis in [8] of the stationary solution of the discrete equations of the numerical method to the theoretical stationary solution of the model (1.4)-(1.6) as established in [9, 11]. Now the novelty is that the approach to the discretization of the model (1.4)-(1.6) proceeds without using the general strategy of considering an artificial truncation of the unbounded age-interval previous to the discretization of the problem. Therefore, the actual asymptotic equilibria solutions of the model (1.4)-(1.6) are approximated, and not the ones derived from the truncated model as reported in [8].

The paper is organized as follows. In the next section, we propose a second order numerical method, described in detail. We carry out an asymptotic analysis about the convergence of the numerical stationary solution to the corresponding theoretical equilibria in section 3. We conclude with a section devoted to numerical experiments that confirm the theoretical results.

2. Numerical approximation

In the following lines, we propose a numerical method to obtain the approximation to the solution of the model (1.4)-(1.6) as described in the introduction. As it was mentioned, the variables involved in the model, both the age, which is the structuring variable, and the time, which describes the evolution of the density of the population are unbounded.

We are going to introduce a numerical scheme to obtain the approximation of the solution in a fixed finite time-interval that we denote as $[0, T]$. The amplitude of such temporal interval is undetermined with its corresponding effect in the convergence error. Regarding the variable that structures the individuals in the population, the discretization techniques require to work in a bounded interval thus far. However, when we follow [2], where we have developed a technique that allows us to propose a numerical method that integrates the model using the unbounded age-interval, we avoid truncating the age-interval as in [8], where a fixed maximum age $A_{\max}$ was introduced to deal with a finite setting in the whole numerical integration.

This technique requires to analyze an artificial size-structured population problem that we obtain after a change of variable in both the dependent and the independent variables. This new model is described as a size-structured

population problem with the size in a bounded interval. The proposed change of variable, which links both structuring variables, is given by $a = \beta(x)$, $\beta(x) = -\frac{1}{K_\beta}\log(1-x)$, and we define $g(x) = 1/\beta'(x)$. The new dependent variables are defined as

$$v(\beta(x),t) = g(x)\, f(x,t), \quad h(\beta(x),t) = g(x)\, m(x,t), \tag{2.1}$$

and satisfy a size-structured population model given by a system of two equations that describes the evolution of both new populations,

$$\begin{cases} f_t(x,t) + (g(x)\, f(x,t))_x + \mu\, f(x,t) &= -E\, H(t)\, f(x,t)\, \chi_{[0,\Lambda]}(x), \\ m_t(x,t) + (g(x)\, m(x,t))_x + \delta\, m(x,t) &= 0, \end{cases} \tag{2.2}$$

$x \in (0,1)$, $t > 0$, where $\Lambda = 1 - \exp(-K_\beta A)$, and the velocity in the rate of change of the new variable is given by the growth rate $g(x) = K_\beta\,(1-x)$ that is the same in both populations. It is completed with the boundary conditions

$$K_\beta\, f(0,t) = 1, \quad K_\beta\, m(0,t) = \int_{\tilde{\Lambda}}^{1} f(x,t)\, dx, \quad t > 0, \tag{2.3}$$

where $\tilde{\Lambda} = 1 - \exp(-K_\beta)$, and the corresponding initial conditions,

$$f(x,0) = f^0(x), \quad m(x,0) = m^0(x), x \in [0,1). \tag{2.4}$$

Due to the fact that $H(t) = \displaystyle\int_0^\infty h(a,t)\, da = \int_0^1 m(x,t)\, dx$, we conserve the same notation to describe the total populations in the new variables.

Once we perform the change of variable, the numerical method we proposed is based on the integration along the characteristics curves in (2.2), which are given by the solution of $x'(t) = g(x(t))$. Therefore, we describe the following integral representation formula of the solution of the model along them,

$$\begin{aligned} f(x(t^*+k), t^*+k) &= f(x(t^*), t^*) \times \\ &\quad \exp\left(-\int_0^k \left(\mu - K_\beta + E\, H(t^*+\tau)\, \chi_{[0,\Lambda]}(x(t^*+\tau))\right) d\tau\right), \end{aligned} \tag{2.5}$$

$$m(x(t^*+k), t^*+k) = m(x(t^*), t^*)\, \exp\left(-(\delta - K_\beta)\, k\right), \tag{2.6}$$

with $0 < x(t^*) < 1$, $0 < t^* < T + k$. The characteristics curves can be computed explicitly due to the suitable formula of the growth rate that is

produced as a consequence of our choice in the change of variable. This explicit expression is given by $x(t) = 1 - e^{-K_\beta\, t}$, and then $g'(x) = -K_\beta$ that is employed in (2.5)-(2.6). In this representation, it is assured that for each $k > 0$ we have $x(t^* + k) < 1$, due to the properties of the growth function.

The numerical method consists in the discretization of (2.5)-(2.6). First, we introduce a grid on the physiologically structured variable but, considering that there exists a discontinuity in the sink term when we arrive at the size $x = \Lambda$ (with corresponding age $a = A$), we will keep localized this jump by setting Λ (A in the age variable) as a node of the grid on the size variable. To this end, given a positive integer J, we define the discretization time parameter as $k = A/J$.

The values of the nodes in the nonuniform grid on size can be explicitly determined using the formula of the characteristics curves. Therefore, they are given by $x_j = 1 - e^{-K_\beta\, k\, j}$, $j \geq 0$. At this point, we must select the last node of the grid in the size variable that we define as x_{J^*}, which is the first node that satisfies

$$1 - x_{J^*} = e^{-K_\beta\, k\, J^*} \leq K\, k,$$

where K is a fixed constant that does not depend on the discretization parameter. For further details we refer to [5, 6, 2]. The selection of the time discretization parameter makes that $x_J = 1 - e^{-K_\beta k\, J} = \Lambda$, *i.e.* the discontinuity point is a node of the grid. With respect to the time discretization variable, we define the discrete time levels as usual, $t_n = n\, k$, $0 \leq n \leq N$, where $N = \lfloor T/k \rfloor$.

Now, we consider that F_j^n and M_j^n represent numerical approximations to $f(x_j, t^n)$ and $m(x_j, t^n)$, respectively, $0 \leq j \leq J^*$, $0 \leq n \leq N$, where the subscript j refers to the grid point x_j and the superscript n to the time level t^n. For convenience, we denote the discrete approximations in vector form: $\mathbf{F}^n = (F_0^n, F_1^n, \ldots, F_{J^*}^n)$, $\mathbf{M}^n = (M_0^n, M_1^n, \ldots, M_{J^*}^n)$, $0 \leq n \leq N$. Thus, once we know initial approximations $\mathbf{F}^0, \mathbf{M}^0 \in \mathbb{R}^{J^*+1}$ to the initial conditions (2.4), which are usually the grid restriction of the initial functions

$$F_j^0 = f^0(x_j), \quad M_j^0 = m^0(x_j), \quad 0 \leq j \leq J^*, \tag{2.7}$$

then the numerical method is defined from the following general recursion that provides the numerical approximation, $(\mathbf{F}^{n+1}, \mathbf{M}^{n+1})$, $0 \leq n \leq N-1$, at the time level t^{n+1} from the approximation, $(\mathbf{F}^n, \mathbf{M}^n)$, at the time level

t^n:

$$F_{j+1}^{n+1} = F_j^n\, e^{(K_\beta-\mu)k} \exp\left(-\frac{k}{2}\, E\, \left(\mathcal{Q}_k(\mathbf{M}^n) + \mathcal{Q}_k(\mathbf{M}^{n+1})\right)\right),$$
$$0 \le j \le J-1, \tag{2.8}$$

$$F_{j+1}^{n+1} = F_j^n\, e^{(K_\beta-\mu)k}, \quad J \le j \le J^*-1, \tag{2.9}$$

$$M_{j+1}^{n+1} = M_j^n\, e^{(K_\beta-\delta)k}, \quad 0 \le j \le J^*-1, \tag{2.10}$$

where, on the one hand, we obtain (2.8) replacing the integral in (2.5) by the trapezoidal quadrature rule, and the integral defining H with the corresponding approximation by means of a quadrature rule. On the other hand, (2.9) and (2.10) are the discrete versions of (2.5) and (2.6), respectively. In general, $\mathcal{Q}_k(\mathbf{U})$ represents a quadrature rule, based on the composite trapezoidal rule with suitable rectangular rules on the first and last intervals, to approximate an integral over the interval $[0,1]$, that can be described as

$$\mathcal{Q}_k(\mathbf{U}) = x_1\, U_1 + \sum_{j=1}^{J^*-1} \frac{x_{j+1}-x_j}{2}\, (U_j + U_{j+1}) + (1-x_{J^*})\, U_{J^*}, \tag{2.11}$$

given $\mathbf{U} = (U_0, U_1, \ldots, U_{J^*})$. This is a second order quadrature rule (we find further details in [2]).

We finish the description of the numerical method with the approximation to the boundary values. The first boundary condition in (2.3) provides the numerical boundary condition

$$F_0^{n+1} = \frac{1}{K_\beta}. \tag{2.12}$$

The second boundary condition (2.3) involves an integral term in which the size at maturity $x = \tilde{\Lambda}$ (the corresponding age value is $a = 1$) is not, in general, a grid point. In order to minimize its impact, let be $\bar{J}$ the first nonnegative integer such that $\tilde{\Lambda} < x_{\bar{J}}$ (and, correspondingly, $1 < \bar{J}\, k$). We have the same purpose as in (2.11). That is why we define the following approximation formula: in the first subinterval $[\tilde{\Lambda}, x_{\bar{J}}]$, we use a rectangular quadrature rule and, for the remaining intervals, a similar quadrature rule as in (2.11), that is

$$M_0^{n+1} = \frac{1}{K_\beta}\left((x_{\bar{J}} - \tilde{\Lambda}) F_{\bar{J}}^{n+1} + \sum_{j=\bar{J}}^{J^*-1} \frac{x_{j+1}-x_j}{2}\left(F_j^{n+1} + F_{j+1}^{n+1}\right) + (1-x_{J^*}) F_{J^*}^{n+1}\right), \tag{2.13}$$

that also represents a second order approximation to the nonlocal term. It is important to notice that the numerical method in (2.7)-(2.13) can be explicitly implemented because $x_J = \Lambda \leq \bar{\Lambda}$. We refer to [8] for further details and a complete description of the problem and its solution with a numerical method that employed a truncated age. Finally, $\mathcal{Q}_k(\mathbf{F}^n)$ and $\mathcal{Q}_k(\mathbf{M}^n)$, provide approximations to the total populations of virgin mictic females and haploid males, $V(t)$ and $H(t)$, respectively, at the time t^n.

Once we get the approximation to the solution in the size-structured population model, we can obtain the corresponding ones to the solution to the original problem. We can consider that $a_j = j\,k$, and V_j^n, H_j^n represent numerical approximations to $v(a_j, t^n)$ and $h(a_j, t^n)$, respectively, $0 \leq j \leq J^*$, $0 \leq n \leq N$. Then, the following formulae define the approximations to the solution to (1.4)-(1.5)

$$V_j^n = K_\beta\, F_j^n\, e^{-K_\beta j k}, \tag{2.14}$$

$$H_j^n = K_\beta\, M_j^n\, e^{-K_\beta j k}. \tag{2.15}$$

We also must point out that since it is unusual to carry out an analysis of convergence of a model with a discontinuous sink term, this should be done very carefully. However, when the vital functions of both populations are smooth enough, the compatibility conditions at $t = 0$ are satisfied, and the (jump) points are represented on the grid, we can employ typical tools and arguments as in [7] that allow us to conclude the second order of convergence of the proposed numerical method.

3. Asymptotic analysis

The asymptotic study of model (1.4)-(1.5) was initiated by Calsina and Ripoll in [11]. In their study, they described the equilibrium solution of the problem. Thus, if H^* denotes the male population at the equilibrium, H^* is the solution to the following transcendental equation

$$\mu\,\delta\,H^* = \mathrm{e}^{-(\mu + E\,H^*\,A)}. \tag{3.1}$$

They showed that equation (3.1) has a unique solution that belongs to the interval $(0, \mathrm{e}^{-\mu}/(\mu\delta))$, for any positive values of μ, δ, E and A. Once this value is obtained, the total population of the virgin females is computed via the following formula,

$$V^* = \frac{\mu + E\,H^*\,\mathrm{e}^{-(\mu + E\,H^*)\,A}}{\mu\,(\mu + E\,H^*)}, \tag{3.2}$$

and, also, the equilibrium solution of both populations in (1.4)-(1.5) as

$$v^*(a) = \begin{cases} e^{-(\mu + E\,H^*)\,a}, & a \in [0, A], \\ e^{-(\mu\,a + E\,H^*\,A)}, & a \in [A, \infty). \end{cases} \tag{3.3}$$

$$h^*(a) = \delta\,H^*\,\mathrm{e}^{-\delta\,a}, \quad a \in [0, \infty). \tag{3.4}$$

They proved the stability of the equilibrium and the existence of a Hopf bifurcation at which the stability of the equilibrium is lost and a stable limit cycle appears. This limit cycle and its period was computed through the linear approximation of the equations (3.1)-(3.4). Later, we performed an analysis to obtain the convergence of a numerical method based on a truncation of the age-interval to better approach the dynamics of the model and the shape and period of the stable limit cycle [8]. Now, we improve the approximation with a numerical method that do not employ the trick of truncating the age-interval.

In the following, we will show how the dynamics of the discrete model (2.8)-(2.10) approach the behavior of the continuous one when the time discretization parameter k is sufficiently small. First, due to the main role that the artificial size-structured population model (2.2)-(2.3) has in our numerical method, we determine the expressions of its steady states in terms of the new variables. Due to the change of the variable, the equilibria of the total populations keep the values H^* and V^*. Then, with respect to the new size-structured populations, the equilibrium solutions are given by

$$f^*(x) = \frac{1}{K_\beta} \begin{cases} (1-x)^{\frac{(\mu + E\,H^*)}{K_\beta} - 1}, & x \in [0, \Lambda], \\ (1-x)^{\frac{\mu}{K_\beta} - 1}\,(1-\Lambda)^{\frac{E\,H^*}{K_\beta}}, & x \in [\Lambda, 1). \end{cases} \tag{3.5}$$

$$m^*(x) = \frac{\delta\,H^*}{K_\beta}(1-x)^{\frac{\delta}{K_\beta} - 1}, \quad x \in [0, 1). \tag{3.6}$$

Now, we describe the equilibrium solution of the numerical method (2.8)-

(2.13). Such solution $(\mathbf{F}, \mathbf{M})$ satisfies

$$F_0 = \frac{1}{K_\beta}, \tag{3.7}$$

$$F_{j+1} = F_j\, e^{(K_\beta-\mu)k} \exp\left(-k\, E\, \mathcal{Q}_k(\mathbf{M})\right), \quad 0 \le j \le J-1, \tag{3.8}$$

$$F_{j+1} = F_j\, e^{(K_\beta-\mu)k}, \quad J \le j \le J^*-1, \tag{3.9}$$

$$M_0 = \frac{1}{K_\beta}\left((x_{\bar{J}} - \tilde{\Lambda})\, F_{\bar{J}} + \sum_{j=\bar{J}}^{J^*-1} \frac{x_{j+1}-x_j}{2}\, (F_j + F_{j+1}) + (1-x_{J^*})\, F_{J^*} \right), \tag{3.10}$$

$$M_{j+1} = M_j\, e^{(K_\beta-\delta)k}, \quad 0 \le j \le J^*-1. \tag{3.11}$$

We would like to mention that we can recover the asymptotic values of the discretization of the original age-structured model from these formulae (3.14)-(3.15) by means of

$$V_j = K_\beta\, F_j\, e^{-K_\beta j k}, \tag{3.12}$$

$$H_j = K_\beta\, M_j\, e^{-K_\beta j k}, \tag{3.13}$$

$0 \le j \le J^*$.

Then, we describe the equilibrium solution of the numerical method in terms of the approach to the total population of males. From (3.7)-(3.9), we obtain

$$F_j = \frac{1}{K_\beta} \begin{cases} e^{\left(K_\beta-\mu-E\,\mathcal{Q}_k(\mathbf{M})\right) j\, k}, & 0 \le j \le J, \\ e^{\left(K_\beta-\mu\right) j\, k} (1-\Lambda)^{\frac{E\,\mathcal{Q}_k(\mathbf{M})}{K_\beta}}, & J+1 \le j \le J^*. \end{cases} \tag{3.14}$$

From equation (3.11)

$$M_j = M_0\, e^{\left(K_\beta-\delta\right) j\, k}, \quad 0 \le j \le J^*. \tag{3.15}$$

Next, we can compute an expression for the approximation to the total number of virgin mictic females, $\mathcal{Q}_k(\mathbf{F})$. It is given by the following quadrature formula associated to the vector $\mathbf{F}$,

$$\mathcal{Q}_k(\mathbf{F}) = x_1\, F_1 + \sum_{j=1}^{J^*-1} \frac{x_{j+1}-x_j}{2}\, (F_j + F_{j+1}) + (1-x_{J^*})\, F_{J^*},$$

then, we substitute (3.14)-(3.15), to obtain

$$
\begin{aligned}
K_\beta\, \mathcal{Q}_k(\mathbf{F}) \;\; = \;\; & \frac{x_1 + x_2}{2}\, e^{\left(K_\beta - \mu - E\, \mathcal{Q}_k(\mathbf{M})\right) k} + \sum_{j=2}^{J} \frac{x_{j+1} - x_{j-1}}{2}\; e^{\left(K_\beta - \mu - E\, \mathcal{Q}_k(\mathbf{M})\right) k\, j} \\
& + (1-\Lambda)^{\frac{E\, \mathcal{Q}_k(\mathbf{M})}{K_\beta}} \sum_{j=J+1}^{J^*-1} \frac{x_{j+1} - x_{j-1}}{2}\, e^{\left(K_\beta - \mu\right) j\, k} \\
& + \left(1 - \frac{x_{J^*-1} + x_{J^*}}{2}\right)\, e^{\left(K_\beta - \mu\right) J^*\, k} (1-\Lambda)^{\frac{E\, \mathcal{Q}_k(\mathbf{M})}{K_\beta}}.
\end{aligned}
$$

Next, we introduce the definition of the grid nodes in this expression, as $x_j = 1 - e^{-K_\beta\, jk}$, $0 \leq j \leq J^*$,

$$
\begin{aligned}
& K_\beta\, \mathcal{Q}_k(\mathbf{F}) = \left(1 - \frac{e^{-2K_\beta k} + e^{-K_\beta k}}{2}\right)\, e^{\left(K_\beta - \mu - E\, \mathcal{Q}_k(\mathbf{M})\right) k} \\
& + \frac{e^{K_\beta k} - e^{-K_\beta k}}{2} \sum_{j=2}^{J} e^{(-\mu - E\, \mathcal{Q}_k(\mathbf{M}))\, k\, j} + (1-\Lambda)^{\frac{E\, \mathcal{Q}_k(\mathbf{M})}{K_\beta}}\, \frac{e^{K_\beta k} - e^{-K_\beta k}}{2} \sum_{j=J+1}^{J^*-1} e^{-\mu\, j\, k} \\
& + \frac{e^{K_\beta k} + 1}{2}\, e^{-\mu\, k\, J^*} (1-\Lambda)^{\frac{E\, \mathcal{Q}_k(\mathbf{M})}{K_\beta}},
\end{aligned}
$$

in which we substitute $1 - \Lambda = e^{-K_\beta\, A}$, to arrive at

$$
\begin{aligned}
K_\beta\, \mathcal{Q}_k(\mathbf{F}) = & \left(e^{K_\beta k} - \frac{e^{-K_\beta k} + 1}{2}\right)\, e^{-(\mu + E\, \mathcal{Q}_k(\mathbf{M}))\, k} \\
& + \frac{e^{K_\beta k} - e^{-K_\beta k}}{2}\, \frac{e^{-(\mu + E\, \mathcal{Q}_k(\mathbf{M}))\, 2k} - e^{-(\mu + E\, \mathcal{Q}_k(\mathbf{M}))\, k(J+1)}}{1 - e^{-(\mu + E\, \mathcal{Q}_k(\mathbf{M}))\, k}} \\
& + (1-\Lambda)^{\frac{E\, \mathcal{Q}_k(\mathbf{M})}{K_\beta}}\, \frac{e^{K_\beta k} - e^{-K_\beta k}}{2}\, \frac{e^{-\mu\,(J+1)\, k} - e^{-\mu\, J^*\, k}}{1 - e^{-\mu\, k}} \\
& + \frac{e^{K_\beta k} + 1}{2}\, e^{-\mu\, k\, J^*} (1-\Lambda)^{\frac{E\, \mathcal{Q}_k(\mathbf{M})}{K_\beta}} \\
= & \frac{e^{K_\beta k} - 1}{2}\, e^{-(\mu + E\, \mathcal{Q}_k(\mathbf{M}))\, k} + \frac{e^{K_\beta k} - e^{-K_\beta k}}{2}\, e^{-(\mu + E\, \mathcal{Q}_k(\mathbf{M}))\, k} \frac{1 - e^{-(\mu + E\, \mathcal{Q}_k(\mathbf{M}))\, A}}{1 - e^{-(\mu + E\, \mathcal{Q}_k(\mathbf{M}))\, k}} \\
& + e^{-\mu}\, (1-\Lambda)^{\frac{E\, \mathcal{Q}_k(\mathbf{M})}{K_\beta}}\, \frac{e^{K_\beta k} - e^{-K_\beta k}}{2}\, \frac{e^{-\mu\, k} - e^{-\mu\,(J^* - J)\, k}}{1 - e^{-\mu\, k}} \\
& + \frac{e^{K_\beta k} + 1}{2}\, e^{-\mu\, k\, (J^* - J)} e^{-\mu}\, (1-\Lambda)^{\frac{E\, \mathcal{Q}_k(\mathbf{M})}{K_\beta}}.
\end{aligned}
$$

Then,

$$\mathcal{Q}_k(\mathbf{F}) = \frac{e^{K_\beta k}-1}{2\,K_\beta}\,e^{-(\mu+E\,\mathcal{Q}_k(\mathbf{M}))\,k} + \frac{e^{K_\beta k}-e^{-K_\beta k}}{2\,K_\beta}\left(\frac{1-e^{-\mu}\,(1-\Lambda)^{\frac{E\,\mathcal{Q}_k(\mathbf{M})}{K_\beta}}}{e^{(\mu+E\,\mathcal{Q}_k(\mathbf{M}))\,k}-1}\right.$$

$$\left.+e^{-\mu}(1-\Lambda)^{\frac{E\,\mathcal{Q}_k(\mathbf{M})}{K_\beta}}\,\frac{1-e^{-\mu\,(J^*-J-1)\,k}}{e^{\mu\,k}-1}\right)+\frac{e^{K_\beta k}+1}{2\,K_\beta}\,e^{-\mu\,k\,(J^*-J)}e^{-\mu}\,(1-\Lambda)^{\frac{E\,\mathcal{Q}_k(\mathbf{M})}{K_\beta}}. \tag{3.16}$$

On the other hand, in a similar way, we can obtain an expression for the numerical value of the total number of haploid males at the equilibrium, $\mathcal{Q}_k(\mathbf{M})$, which is given by the quadrature formula associated with the vector $\mathbf{M}$,

$$\begin{aligned}\mathcal{Q}_k(\mathbf{M}) &= x_1\,M_1+\sum_{j=1}^{J^*-1}\frac{x_{j+1}-x_j}{2}\,(M_j+M_{j+1})+(1-x_{J^*})\,M_{J^*}\\ &= \frac{x_1+x_2}{2}\,M_1+\sum_{j=2}^{J^*-1}\frac{x_{j+1}-x_{j-1}}{2}M_j+\left(1-\frac{x_{J^*-1}+x_{J^*}}{2}\right)\,M_{J^*}.\end{aligned}$$

Then, we substitute (3.15), and the definition of the grid nodes in this expression, as $x_j = 1-e^{-K_\beta\,jk}$, $0\le j\le J^*$, to arrive at

$$\begin{aligned}\mathcal{Q}_k(\mathbf{M}) &= M_0\,\left(\left(1-\frac{e^{-K_\beta k}-e^{-K_\beta 2k}}{2}\right)e^{K_\beta k}e^{-\delta\,k}\right.\\ &\quad\left.+\sum_{j=2}^{J^*-1}e^{-K_\beta kj}\frac{e^{K_\beta k}-e^{-K_\beta k}}{2}e^{K_\beta kj}e^{-\delta\,kj}+e^{-K_\beta kJ^*}\frac{1+e^{K_\beta k}}{2}e^{K_\beta kJ^*}e^{-\delta\,kJ^*}\right)\\ &= M_0\,\left(\left(1-\frac{e^{-K_\beta k}-e^{-K_\beta 2k}}{2}\right)e^{K_\beta k}e^{-\delta\,k}+\frac{e^{K_\beta k}-e^{-K_\beta k}}{2}\frac{e^{-\delta\,2k}-e^{-\delta\,kJ^*}}{1-e^{-\delta\,k}}\right.\\ &\quad\left.+\frac{1+e^{K_\beta k}}{2}e^{-\delta\,kJ^*}\right)\\ &= M_0\,\left(\frac{e^{K_\beta k}-1}{2}e^{-\delta\,k}+\frac{e^{K_\beta k}-e^{-K_\beta k}}{2}\frac{e^{-\delta\,k}-e^{-\delta\,kJ^*}}{1-e^{-\delta\,k}}+\frac{1+e^{K_\beta k}}{2}e^{-\delta\,kJ^*}\right)\\ &= M_0\,\left(\frac{e^{K_\beta k}-1}{2}e^{-\delta\,k}+\frac{e^{K_\beta k}-e^{-K_\beta k}}{2}\frac{1-e^{-\delta\,kJ^*}}{e^{\delta\,k}-1}+\frac{1+e^{-K_\beta k}}{2}e^{-\delta\,kJ^*}\right).\end{aligned}$$

Now, we define δ_k as the following formula,

$$\delta_k := \frac{K_\beta}{\frac{e^{K_\beta k}-1}{2}e^{-\delta\, k} + \frac{e^{K_\beta k}-e^{-K_\beta k}}{2}\frac{1-e^{-\delta\, k J^*}}{e^{\delta\, k}-1} + \frac{1+e^{-K_\beta k}}{2}e^{-\delta\, k J^*}}. \tag{3.17}$$

Note that δ_k is only depending on the time discretization parameter (k), and, also, on the parameters K (through J^*) and K_β of the numerical procedure. In fact, we subsequently prove that δ_k represents a numerical approximation to the mortality rate of the individuals in the male population. It means that

$$K_\beta\, M_0 = \delta_k\, \mathcal{Q}_k(\mathbf{M}), \tag{3.18}$$

and we substitute this expression in (3.15) to obtain

$$M_j = \frac{\delta_k}{K_\beta}\, \mathcal{Q}_k(\mathbf{M})\, e^{\left((K_\beta-\delta)\, j\, k\right)}, \quad 0 \le j \le J^*.$$

Now, formula in (3.10) defines M_0 in a different way

$$K_\beta M_0 = (x_{\bar{J}} - \tilde{\Lambda})\, F_{\bar{J}} + \sum_{j=\bar{J}}^{J^*-1} \frac{x_{j+1}-x_j}{2}\, (F_j + F_{j+1}) + (1 - x_{J^*})\, F_{J^*},$$

in which, first, we substitute (3.14), to have

$$\begin{aligned} K_\beta^2\, M_0 = &\left(\frac{x_{\bar{J}+1}+x_{\bar{J}}}{2} - \tilde{\Lambda}\right) e^{K_\beta\, \bar{J}k} e^{-\mu\, \bar{J}k}\, (1-\Lambda)^{\frac{E\, \mathcal{Q}_k(\mathbf{M})}{K_\beta}} \\ &+ (1-\Lambda)^{\frac{E\, \mathcal{Q}_k(\mathbf{M})}{K_\beta}} \sum_{j=\bar{J}+1}^{J^*-1} \frac{x_{j+1}-x_{j-1}}{2}\, e^{K_\beta\, kj}\, e^{-\mu\, k\, j} \\ &+ \left(1 - \frac{x_{J^*-1}+x_{J^*}}{2}\right) e^{K_\beta\, J^*\, k} e^{-\mu\, J^*\, k} (1-\Lambda)^{\frac{E\, \mathcal{Q}_k(\mathbf{M})}{K_\beta}}, \end{aligned}$$

and, then, the definition of the grid nodes in this expression, as $x_j = 1 -$

$e^{-K_\beta\, jk}$, $0 \le j \le J^*$, to arrive at

$$
\begin{aligned}
K_\beta^2\, M_0\, e^{\mu}\, (1-\Lambda)^{-\frac{E\,\mathcal{Q}_k(\mathbf{M})}{K_\beta}} = & \left(1-\tilde{\Lambda}-\frac{e^{-K_\beta \bar{J} k}+e^{-K_\beta(\bar{J}+1)k}}{2}\right) e^{K_\beta\, \bar{J} k} e^{-\mu\,(\bar{J}-J)\,k} \\
& + \frac{e^{K_\beta k}-e^{-K_\beta k}}{2} \sum_{j=\bar{J}+1}^{J^*-1} e^{-\mu\, k\,(j-J)} + \frac{e^{K_\beta k}+1}{2}\, e^{-\mu\, k\,(J^*-J)} \\
= & \left(\left(1-\tilde{\Lambda}\right) e^{K_\beta\, \bar{J} k} - \frac{1+e^{-K_\beta k}}{2}\right) e^{-\mu\,(\bar{J}-J)\,k} \\
& + \frac{e^{K_\beta k}-e^{-K_\beta k}}{2}\, \frac{e^{-\mu\, k\,(\bar{J}-J+1)}-e^{-\mu\, k\,(J^*-J)}}{1-e^{-\mu\, k}} + \frac{e^{K_\beta k}+1}{2}\, e^{-\mu\, k\,(J^*-J)}.
\end{aligned}
$$

Now, we define μ_k as the following expression

$$
\begin{aligned}
\frac{K_\beta}{\mu_k} := & \left(\left(1-\tilde{\Lambda}\right) e^{K_\beta\, \bar{J} k} - \frac{1+e^{K_\beta k}}{2}\right) e^{-\mu\,(\bar{J}-J)\,k} \\
& + \frac{e^{K_\beta k}-e^{-K_\beta k}}{2}\, \frac{e^{-\mu\, k\,(\bar{J}-J)}-e^{-\mu\, k\,(J^*-J)}}{1-e^{-\mu\, k}} + \frac{e^{K_\beta k}+1}{2}\, e^{-\mu\, k\,(J^*-J)},
\end{aligned}
$$

in which, again, we emphasize the dependency on all the discretization parameters, not only the time discretization parameter k, but also the parameters K and K_β in the numerical procedure. In fact, we subsequently prove that μ_k represents a numerical approximation to the value of the mortality for the individual female population. Therefore,

$$
K_\beta\, \mu_k\, M_0 = e^{-\mu}\, (1-\Lambda)^{\frac{E\,\mathcal{Q}_k(\mathbf{M})}{K_\beta}},
$$

and, with the use of (3.18), a transcendental equation for the total population of haploid males just involving the parameters of the problem is obtained,

$$
\delta_k\, \mu_k\, \mathcal{Q}_k(\mathbf{M}) = e^{-\mu}\, (1-\Lambda)^{\frac{E\,\mathcal{Q}_k(\mathbf{M})}{K_\beta}}. \tag{3.19}
$$

The following result shows that the equilibrium solution of the numerical method (3.7)-(3.11) converges to the equilibrium solution of the problem (2.2)-(2.3) as k tends to zero. More precisely, the convergence is of second order.

Theorem 1. *For any positive values μ, δ, E and A, let H^* denote the unique positive solution of (3.1), and let V^*, f^* and m^* be defined by (3.2), (3.5)*

and (3.6), respectively. For any $k > 0$, let $\mathcal{Q}_k(\mathbf{M})$ denote the unique positive solution of (3.19), and let $\mathcal{Q}_k(\mathbf{F})$, $\mathbf{M}$ and $\mathbf{F}$ be defined by (3.16), (3.15) and (3.14), respectively. Then, as $k \to 0$,

$$\begin{aligned} |H^* - \mathcal{Q}_k(\mathbf{M})| &= \mathcal{O}(k^2), && (3.20)\\ |V^* - \mathcal{Q}_k(\mathbf{F})| &= \mathcal{O}(k^2), && (3.21)\\ |f^*(x_j) - F_j| &= \mathcal{O}(k^2), \quad 0 \le j \le J^*, && (3.22)\\ |m^*(x_j) - M_j| &= \mathcal{O}(k^2), \quad 0 \le j \le J^*. && (3.23) \end{aligned}$$

Proof We first deal with the existence and uniqueness of a solution of (3.19). Then we define the function

$$\Phi(x) = \delta_k \, \mu_k \, e^{\mu} \, x \, e^{E \, A \, x} - 1.$$

This function is continuous and increasing and its value at $x = 0$ is negative, then there exists a unique solution of the equation $\Phi(x) = 0$. As we show that $\mathcal{Q}_k(\mathbf{M})$ satisfies this equation, we find that this value is the unique solution of (3.19).

On the other hand, the following expresion comes from the chosen change of variable

$$1 = \delta \int_0^\infty e^{-\delta \, a} \, da = \frac{\delta}{K_\beta} \int_0^1 (1-x)^{\frac{\delta}{K_\beta}-1} \, dx. \tag{3.24}$$

Also, the properties of the quadrature rule ensure that

$$\begin{aligned} &\int_0^1 (1-x)^{\frac{\delta}{K_\beta}-1} \, dx = x_1 \, (1-x_1)^{\frac{\delta}{K_\beta}-1} \\ &\quad + \sum_{j=2}^{J^*} \frac{x_j - x_{j-1}}{2} \left((1-x_{j-1})^{\frac{\delta}{K_\beta}-1} + (1-x_j)^{\frac{\delta}{K_\beta}-1} \right) + (1-x_{J^*})^{\frac{\delta}{K_\beta}} + \mathcal{O}(k^2). \\ &= \frac{x_1 + x_2}{2} \, (1-x_1)^{\frac{\delta}{K_\beta}-1} + \sum_{j=2}^{J^*-1} \frac{x_{j+1} - x_{j-1}}{2} (1-x_j)^{\frac{\delta}{K_\beta}-1} \\ &\quad + \frac{x_{J^*} - x_{J^*-1}}{2} (1-x_{J^*})^{\frac{\delta}{K_\beta}} + \mathcal{O}(k^2). \end{aligned}$$

Now, we employ the definition of the grid nodes in this expression, as $x_j =$

$1 - e^{-K_\beta\, jk}$, $0 \leq j \leq J^*$, to arrive at

$$\begin{aligned}
\int_0^1 (1-x)^{\frac{\delta}{K_\beta}-1}\, dx &= \left(1 - e^{-K_\beta k}\right) e^{-\delta\, k} e^{K_\beta k} \\
&\quad + \frac{1}{2}\left(e^{K_\beta k} - 1\right)\left(1 + e^{(\delta - K_\beta)k}\right) \sum_{j=2}^{J^*} e^{-\delta\, k\, j} + e^{-\delta\, k\, J^*} + \mathcal{O}(k^2) \\
&= \left(e^{K_\beta k} - 1\right) e^{-\delta\, k} + \frac{1}{2}\left(1 - e^{-K_\beta k}\right)\left(e^{K_\beta\, k} + e^{\delta\, k}\right) \frac{e^{-2\delta\, k} - e^{-\delta\, k\,(J^*+1)}}{1 - e^{-\delta\, k}} \\
&\quad + e^{-\delta\, k\, J^*} + \mathcal{O}(k^2) \qquad (3.25) \\
&= \frac{1}{2}\left(e^{K_\beta k} - 1\right) e^{-\delta\, k} + \frac{1}{2}\left(e^{K_\beta k} - 1\right) \frac{e^{-\delta\, k} - e^{-\delta\, k\,(J^*+1)}}{1 - e^{-\delta\, k}} \\
&\quad + \frac{1}{2}\left(1 - e^{-K_\beta k}\right) \frac{e^{-\delta\, k} - e^{-\delta\, k\, J^*}}{1 - e^{-\delta\, k}} + e^{-\delta\, k\, J^*} + \mathcal{O}(k^2) \\
&= \frac{1}{2}\left(e^{K_\beta k} - 1\right) e^{-\delta\, k} + \frac{1}{2}\left(e^{K_\beta k} - e^{-K_\beta k}\right) \frac{1 - e^{-\delta\, k\, J^*}}{e^{\delta\, k} - 1} \\
&\quad + \frac{1}{2}\left(1 - e^{-K_\beta k}\right) \frac{e^{-\delta\, k\,(J^*+1)} - e^{-\delta\, k\, J^*}}{1 - e^{-\delta\, k}} + e^{-\delta\, k\, J^*} + \mathcal{O}(k^2) \\
&= \frac{1}{2}\left(e^{K_\beta k} - 1\right) e^{-\delta\, k} + \frac{1}{2}\left(e^{K_\beta k} - e^{-K_\beta k}\right) \frac{1 - e^{-\delta\, k\, J^*}}{e^{\delta\, k} - 1} \\
&\quad + \frac{1}{2}\left(1 + e^{-K_\beta k}\right) e^{-\delta\, k\, J^*} + \mathcal{O}(k^2) \\
&= \frac{K_\beta}{\delta_k} + \mathcal{O}(k^2). \qquad (3.26)
\end{aligned}$$

Thus, we combine (3.24) with (3.26) to obtain

$$\delta = \delta_k + \mathcal{O}(k^2). \qquad (3.27)$$

We can also follow similar steps with the following integral,

$$1 = e^{\mu}\mu \int_1^\infty e^{-\mu\, a}\, da = \frac{e^{\mu}\mu}{K_\beta} \int_{\tilde{\Lambda}}^1 (1-x)^{\frac{\mu}{K_\beta}-1}\, dx. \qquad (3.28)$$

In which we can also apply the properties of the quadrature rule and ensure

that

$$\int_{\tilde{\Lambda}}^{1} (1-x)^{\frac{\mu}{K_\beta}-1}\,dx = (x_{\bar{J}} - \tilde{\Lambda})\,(1-x_{\bar{J}})^{\frac{\mu}{K_\beta}-1}$$
$$+ \sum_{j=\bar{J}+1}^{J^*} \frac{x_j - x_{j-1}}{2}\left((1-x_{j-1})^{\frac{\mu}{K_\beta}-1} + (1-x_j)^{\frac{\mu}{K_\beta}-1}\right) + (1-x_{J^*})^{\frac{\mu}{K_\beta}} + \mathcal{O}(k^2).$$

Then, we substitute the expression of the grid nodes, and we use the definition of F^* to obtain

$$\begin{aligned}
\int_{\tilde{\Lambda}}^{1} (1-x)^{\frac{\mu}{K_\beta}-1}\,dx &= (1 - e^{-K_\beta\, k\, \bar{J}} - \tilde{\Lambda})\, e^{(K_\beta-\mu)\, k\, \bar{J}} \\
&\quad + \frac{1}{2}\left(e^{K_\beta k} - 1\right)\left(1 + e^{(\mu - K_\beta)k}\right) \sum_{j=\bar{J}+1}^{J^*} e^{-\mu\, k\, j} + e^{-\mu\, k\, J^*} + \mathcal{O}(k^2) \\
&= (1-\tilde{\Lambda})\, e^{(K_\beta-\mu)\, k\, \bar{J}} - e^{-\mu\, k\, \bar{J}} \\
&\quad + \frac{1}{2}\left(e^{K_\beta k} - 1\right)\left(1 + e^{-K_\beta\, k}\, e^{\mu\, k}\right) \frac{e^{-(\bar{J}+1)\mu\, k} - e^{-\mu\, k\, (J^*+1)}}{1 - e^{-\mu\, k}} \\
&\quad + e^{-\mu\, k\, J^*} + \mathcal{O}(k^2) \\
&= (1-\tilde{\Lambda})\, e^{(K_\beta-\mu)\, k\, \bar{J}} - e^{-\mu\, k\, \bar{J}} + \frac{1}{2}\left(e^{K_\beta k} - 1\right) \frac{e^{-(\bar{J}+1)\, \mu\, k} - e^{-(J^*+1)\mu\, k}}{1 - e^{-\mu\, k}} \\
&\quad + \frac{1}{2}\left(1 - e^{-K_\beta k}\right) \frac{e^{-\bar{J}\, \mu\, k} - e^{-\mu\, k\, J^*}}{1 - e^{-\mu\, k}} + e^{-\delta\, k\, J^*} + \mathcal{O}(k^2) \\
&= (1-\tilde{\Lambda})\, e^{(K_\beta-\mu)\, k\, \bar{J}} - \frac{1}{2}\left(e^{K_\beta k} + 1\right) e^{-\mu\, k\, \bar{J}} \\
&\quad + \frac{1}{2}\left(e^{K_\beta k} - e^{-K_\beta k}\right) \frac{e^{-\mu\, k\, \bar{J}} - e^{-\mu\, k\, J^*}}{1 - e^{-\mu\, k}} + \frac{1}{2}\left(1 + e^{K_\beta k}\right) e^{-\mu\, k\, J^*} + \mathcal{O}(k^2) \\
&= \frac{K_\beta}{\mu_k}\, e^{-\mu} + \mathcal{O}(k^2). \qquad (3.29)
\end{aligned}$$

Therefore, we combine (3.28) with (3.29) to arrive at

$$\mu = \mu_k + \mathcal{O}(k^2). \qquad (3.30)$$

Next, the mean value theorem applied to Φ^{-1}, whose derivative is always lower than one, equation (3.1) and approximations (3.27), and (3.30), allow

us to obtain the bound (3.20) because

$$\begin{aligned} |H^* - \mathcal{Q}_k(\mathbf{M})| &\leq |\Phi(H^*)| = |\delta_k\,\mu_k\,e^{\mu}\,H^*\,e^{E\,A\,H^*} - 1| = \frac{1}{\mu\,\delta}|\delta_k\,\mu_k - \delta\,\mu| \\ &\leq C\,k^2. \end{aligned}$$

Next, for $0 \leq j \leq J$, (3.5), and (3.14), the definition of the change of variable, $a = \beta(x)$, and the grid nodes x_j, and (3.20), are enough to prove

$$\begin{aligned} |f^*(x_j) - F_j| &= \left|\frac{1}{K_\beta}(1-x_j)^{\frac{(\mu+E\,H^*)}{K_\beta}-1} - \frac{1}{K_\beta}e^{\left(K_\beta-\mu-E\,\mathcal{Q}_k(\mathbf{M})\right)j\,k}\right| \\ &= \frac{e^{-\left(\mu-K_\beta\right)j\,k}}{K_\beta}\left|e^{-E\,H^*\,j\,k} - e^{-E\,\mathcal{Q}_k(\mathbf{M})\,j\,k}\right| \\ &\leq \frac{E\,j\,k\,e^{-\left(\mu-K_\beta\right)j\,k}}{K_\beta}\,|H^* - \mathcal{Q}_k(\mathbf{M})| \leq C\,k^2. \end{aligned}$$

With the same arguments, for $J+1 \leq j \leq J^*$, we arrive at

$$\begin{aligned} |f^*(x_j) - F_j| &= \left|\frac{1}{K_\beta}(1-x_j)^{\frac{\mu}{K_\beta}-1}\,(1-\Lambda)^{\frac{E\,H^*}{K_\beta}} - \frac{1}{K_\beta}e^{\left(K_\beta-\mu\right)j\,k}(1-\Lambda)^{\frac{E\,\mathcal{Q}_k(\mathbf{M})}{K_\beta}}\right| \\ &= \frac{e^{\left(K_\beta-\mu\right)j\,k}}{K_\beta}\left|e^{-E\,H^*\,A} - e^{-E\,\mathcal{Q}_k(\mathbf{M})\,A}\right| \\ &\leq \frac{e^{\left(K_\beta-\mu\right)j\,k}E\,A}{K_\beta}\,|H^* - \mathcal{Q}_k(\mathbf{M})| \leq C\,k^2. \end{aligned}$$

Thus, we obtain (3.22).

Now, we use (3.6), and (3.15), the definition of the change of variable, $\beta(x)$, and the grid nodes x_j, the relationships (3.18), and (3.27), and (3.20) to obtain

$$\begin{aligned} |m^*(x_j) - M_j| &= \left|\frac{\delta\,H^*}{K_\beta}(1-x_j)^{\frac{\delta}{K_\beta}-1} - M_0\,e^{\left(K_\beta-\delta\right)j\,k}\right| \\ &= \frac{e^{\left(K_\beta-\delta\right)j\,k}}{K_\beta}\,|(\delta-\delta_k)\;H^* + \delta_k\,(H^* - \mathcal{Q}_k(\mathbf{M}))| = \mathcal{O}(k^2), \end{aligned}$$

$J+1 \leq j \leq J^*$, which confirms (3.23).

All in all, (3.21) is demonstrated considering that

$$V^* = \int_0^\infty v^*(a)\,da = \int_0^1 f^*(a)\,da = \mathcal{Q}_k(\mathbf{f}^*) + \mathcal{O}(k^2),$$

and, due to (3.22)

$$\mathcal{Q}_k(\mathbf{f}^*) - \mathcal{Q}_k(\mathbf{F}) = \mathcal{O}(k^2),$$

where $\mathbf{f}^* = (f^*(x_0), f^*(x_1), \ldots, f^*(x_{J^*}))$. □

From this theorem, the following one is immediately obtained, that describes the second order of convergence to the asymptotic state of the original age-structured functions for both haploid males and virgin females.

Theorem 2. *For any positive values μ, δ, E and A, let H^* denote the unique positive solution of (3.1), and let h^* and v^* be defined by (3.4) and (3.3), respectively. For any $k > 0$, let $\mathcal{Q}_k(\mathbf{M})$ denote the unique positive solution of (3.19), and let $\mathbf{H}$ and $\mathbf{V}$ be defined by (3.13), and (3.12), respectively. Then, as $k \to 0$,*

$$|v^*(a_j) - V_j| = \mathcal{O}(k^2), \quad 0 \le j \le J^*, \tag{3.31}$$

$$|h^*(a_j) - H_j| = \mathcal{O}(k^2), \quad 0 \le j \le J^*. \tag{3.32}$$

Proof We only sketch the proof of (3.31), because both are similar. Therefore, the definitions (3.3) and (3.4), allow us to get the relationship

$$v^*(a_j) = K_\beta e^{-K_\beta\, j\, k}\, f^*(x_j), \quad 0 \le j \le J^*,$$

and with equations (3.12), and (3.22), we arrive at the desired result,

$$|v^*(a_j) - V_j| = K_\beta e^{-K_\beta\, j\, k} |f^*(x_j) - F_j|.$$

□

4. Numerical results

In this section, we show the interest of the numerical method presented for the simulation of the sexual phase of the *Monogonont rotifera*. To do this, we compare the behavior of the numerical solution with the theoretical analysis provided by Calsina and Ripoll [11]. In their work, they prove that the model system has a unique stationary population density which is stable as long as a parameter, related to male-female encounter rate, remains below

a critical value. When the parameter increases beyond this critical value, the stationary solution becomes unstable and a stable limit cycle (isolated periodic orbit) appears.

Our aim in this section is to show that the proposed scheme is able to simulate the behavior of the solution that the theoretical analysis predicts for such model. That is, considering the rich dynamics of the problem we show the good behavior of the numerical approximation for long-time simulations. In this paper, as the discretization parameter decreases to zero, we approximate the asymptotic steady solutions for the model problem without previously considering a truncation of the age interval as it was in [8]. We have dealt with two numerical tests taken from the analytical study of the dynamics in Calsina and Ripoll [11]. Both experiments are representative cases of the two possible situations: the stable and the unstable case.

In the first experiment, we consider the reference values $\mu = 0.4$, $\delta = 0.7$, $E = 1.44$ and $A = 0.3$ corresponding to realistic biological data. These are the parameters (using the new units) for some rotifer species belonging to the genera Brachionus [9, 11]. When considering a bifurcation analysis as the parameter E in the model (the male-female encounter rate) varies, Calsina and Ripoll [11] report an instability threshold value at $E_{\text{un}} = 1617.928392$. For parameter values below this critical one the population densities evolve towards the asymptotically stable equilibrium defined by (3.3)-(3.4), with H^* the positive solution of (3.1). In this case, using a nonlinear solver package, we get $H^* = 1.341202$ and then, from (3.2), $V^* = 1.458016$.

We have performed simulations with different values of the parameters K, K_β, and J ($k = A/J$, is the time discretization parameter), in which it is shown how the numerical computation of both, the total population of males and the total population of females, evolve towards and equilibrium, $\mathcal{Q}_k(\mathbf{M})$ and $\mathcal{Q}_k(\mathbf{F})$, respectively. In the experiment, the approximations at $T = 300$ are compared with the theoretical ones, the total population of males and females in the equilibrium solution of the original problem (1.4)-(1.5), H^* defined by (3.1), and V^* defined by (3.2), and the error is measured as

$$e_k = \max\{|\mathcal{Q}_k(\mathbf{M}) - H^*|, |\mathcal{Q}_k(\mathbf{F}) - V^*|\},$$

for each value of the time discretization parameter k, once the other parameters K, K_β, and $A_{\max}$ are fixed in the numerical procedure at each case. The initial conditions considered in the numerical integration are the restriction

to the grid points of the functions

$$v_0(a) = \begin{cases} \mathrm{e}^{-\mu\frac{a}{1-a}}, & a \in [0,1), \\ 0, & a \geq 1, \end{cases} \tag{4.1}$$

$$h_0(a) = 0, \quad a \geq 0, \tag{4.2}$$

that corresponds to a biological initial stage in which there is not haploid males, as it is the case for the starting situation of the sexual phase.

In Tables 1-2, we show numerical results for time discretization parameter $k = 5 \cdot 10^{-2}$, $k = 2.5 \cdot 10^{-2}$, $k = 1.25 \cdot 10^{-2}$, $k = 6.25 \cdot 10^{-3}$, $k = 3.125 \cdot 10^{-3}$, $k = 1.5625 \cdot 10^{-3}$. At each experiment, it is presented the error, e_k, the time of computation in seconds, and the numerical order s as computed from

$$s = \frac{\log e_{2\,k}/e_k}{\log 2}.$$

Table 1 is devoted to the new numerical method with the following couples of parameter values $K = 1$, $K_\beta = 0.7$; $K = 1$, $K_\beta = 0.35$; and $K = 1$, $K_\beta = 0.175$; while Table 2 shows the experiments performed with the numerical method that employs a truncation in the age interval, where we show $A_{\max} = 35$, $A_{\max} = 45$, and $A_{\max} = 50$.

The results shown in Table 1 confirm the asymptotic behavior of the numerical method and the second order of convergence of the numerical to the theoretical steady states as it was predicted in Theorem 2. We show that is important to fulfill the requirements of the convergence theorem [2] that are not satisfied in case of $K_\beta = 0.7$ where the convergence with the expected order fails. However, numerical evidence shows that is enough for convergence to choose $K_\beta = \min\{0.7, 0.4\}$ just to capture the exponential rate of decay with age of the theoretical solution of the problem. Also, in the third column, we manifest that the choice of the parameter K_β, which performs the change of variable, is crucial because we increase the cost without the corresponding effect in the error. With respect to the results shown in Table 2, we also confirm the asymptotic behavior of the numerical method and the second order of convergence of the numerical to the theoretical steady states as it was predicted in [8]. In this case, the choice of the truncation parameter, $A_{\max}$ is important. On one hand, if it is too short, we could saturate the error soon, as we see in the case of $A_{\max} = 35$. On the other hand, the use

k	$K=1,\ K_\beta=0.7$	$K=1,\ K_\beta=0.35$	$K=1,\ K_\beta=0.175$
$5\cdot10^{-2}$	$3.5343491\cdot10^{-3}$	$1.8855845\cdot10^{-4}$	$2.0189815\cdot10^{-4}$
	$4.40510\cdot10^{-1}$	$4.77965\cdot10^{-1}$	$6.54907\cdot10^{-1}$
$2.5\cdot10^{-2}$	$2.3792497\cdot10^{-3}$	$4.6690978\cdot10^{-5}$	$5.0569882\cdot10^{-5}$
	$9.18715\cdot10^{-1}$ 0.57	1.48638 2.01	2.55776 2.00
$1.25\cdot10^{-2}$	$1.6044969\cdot10^{-3}$	$1.1380311\cdot10^{-5}$	$1.2809986\cdot10^{-5}$
	3.10949 0.57	4.88814 2.04	$1.41136\cdot10^{1}$ 1.98
$6.25\cdot10^{-3}$	$1.0805474\cdot10^{-3}$	$2.6773591\cdot10^{-6}$	$3.1846739\cdot10^{-6}$
	$1.10310\cdot10^{1}$ 0.57	$2.81737\cdot10^{1}$ 2.09	$5.26242\cdot10^{1}$ 2.01
$3.125\cdot10^{-3}$	$7.2720506\cdot10^{-4}$	$5.9497584\cdot10^{-7}$	$8.0364412\cdot10^{-7}$
	$6.12610\cdot10^{1}$ 0.57	$1.14004\cdot10^{2}$ 2.17	$2.10902\cdot10^{2}$ 1.99
$1.5625\cdot10^{-3}$	$4.8928730\cdot10^{-4}$	$1.2306731\cdot10^{-7}$	$1.9941992\cdot10^{-7}$
	$2.43243\cdot10^{2}$ 0.57	$4.58032\cdot10^{2}$ 2.27	$7.62861\cdot10^{2}$ 2.01

Table 1: $T = 300$. Results performed with the numerical method in an unbounded age-interval. e_k, time of computation in seconds, and convergence order.

k	$A_{\max}=35$	$A_{\max}=45$	$A_{\max}=50$
$5\cdot10^{-2}$	$2.0164350\cdot10^{-5}$	$2.0711197\cdot10^{-5}$	$2.0719998\cdot10^{-5}$
	4.46875	5.53125	6.32813
$2.5\cdot10^{-2}$	$5.3584525\cdot10^{-6}$	$5.2052835\cdot10^{-6}$	$5.2140847\cdot10^{-6}$
	$1.75938\cdot10^{1}$ 1.91	$2.25625\cdot10^{1}$ 1.99	$2.57031\cdot10^{1}$ 1.99
$1.25\cdot10^{-2}$	$7.3884902\cdot10^{-7}$	$1.2848417\cdot10^{-6}$	$1.2936448\cdot10^{-6}$
	$7.08125\cdot10^{1}$ 2.86	$8.75938\cdot10^{1}$ 2.02	$1.00438\cdot10^{2}$ 2.01
$6.25\cdot10^{-3}$	$9.9837920\cdot10^{-7}$	$3.1956291\cdot10^{-7}$	$3.2836606\cdot10^{-7}$
	$2.76313\cdot10^{2}$ -0.434	$3.57578\cdot10^{2}$ 2.01	$3.96109\cdot10^{2}$ 1.98
$3.125\cdot10^{-3}$	$1.0197689\cdot10^{-6}$	$7.0756015\cdot10^{-8}$	$7.9559683\cdot10^{-8}$
	$1.10763\cdot10^{3}$ -0.0306	$1.41908\cdot10^{3}$ 2.18	$1.57620\cdot10^{3}$ 2.05
$1.5625\cdot10^{-3}$	$1.0500887\cdot10^{-6}$	$1.5821398\cdot10^{-8}$	$2.0731288\cdot10^{-8}$
	$4.48052\cdot10^{3}$ -0.0423	$5.69825\cdot10^{3}$ 2.16	$6.32439\cdot10^{3}$ 1.94

Table 2: $T = 300$. Numerical method with truncation [8]. e_k, time of computation in seconds, and convergence order.

of larger values increases the computational cost without the corresponding effect on the computed error. We have employed other values of parameters K and K_β, and $A_{\max}$ with similar results.

In Figure 1, we compare the efficiency among both methods: firstly, the numerical method based on the discretization of the problem over a truncated age-interval $[0, A_{\max}]$; secondly, the numerical method described in this paper. The global errors versus the times of computation in logarithm scale are shown. We represent all the experiments with the new numerical technique in a (red) straight line and the numerical method provided in [8] with a (black) dashed line. We show that the numerical method described in this paper present the most efficient combination with parameters $K = 1$, $K_\beta = 0.35$. The value of K_β has a clear influence on the efficiency due to the increment on the cost of the computation of the natural grid employed in the artificial size-structured model as K_β is increased. We can also point out that, as we have previously noted, the choice of K_β must satisfy the requirements of convergence theorem [2], otherwise ($K_\beta = 0.7$) convergence is not guaranteed. For a fixed value of K_β and a given value of the global error, decreasing values of K increase the size of the natural grid. However, the parameter K has a lower overall effect than K_β on the computational cost. With respect to the truncated age-interval numerical method, the choice of the value of the $A_{\max}$ is important because an experiment with a short value can saturate the computational error soon, and the choice of a larger value of $A_{\max}$ does not improve its efficiency.

In a second experiment, we use $\mu = 0.9355$, $\delta = 1.4463$, $E = 675.84$ and $A = 0.4274$, the instability threshold value of the encounter rate is minimal, $E_{\text{un}} = 501.831883$ [11]. It means that the reference value $E = 675.84$ makes the equilibrium unstable and a Hopf-bifurcation appears. The equilibrium of (1.4)-(1.5) is defined by (3.3)-(3.4), with $H^* = 0.0112499$ (note that this is a rounded value obtaining by using a nonlinear solver package to (3.1)). From (3.2) we get $V^* = 0.141869$. We do not expect that the reported results were quite different than the ones proposed in [8], however we include them to emphasize that the new numerical method is not based on a truncation of the age domain.

We employ the value $J = 20$ that defines the step size, that is, $k = 2.137 \cdot 10^{-2}$, and the parameters $K = 0.01$, and $K_\beta = 0.1$. In Fig. 2, we show the evolution along the time of both populations, starting from the initial condition (4.1)-(4.2), by means of its trajectory in the phase plane (H, V) that is attracted to a limit cycle.

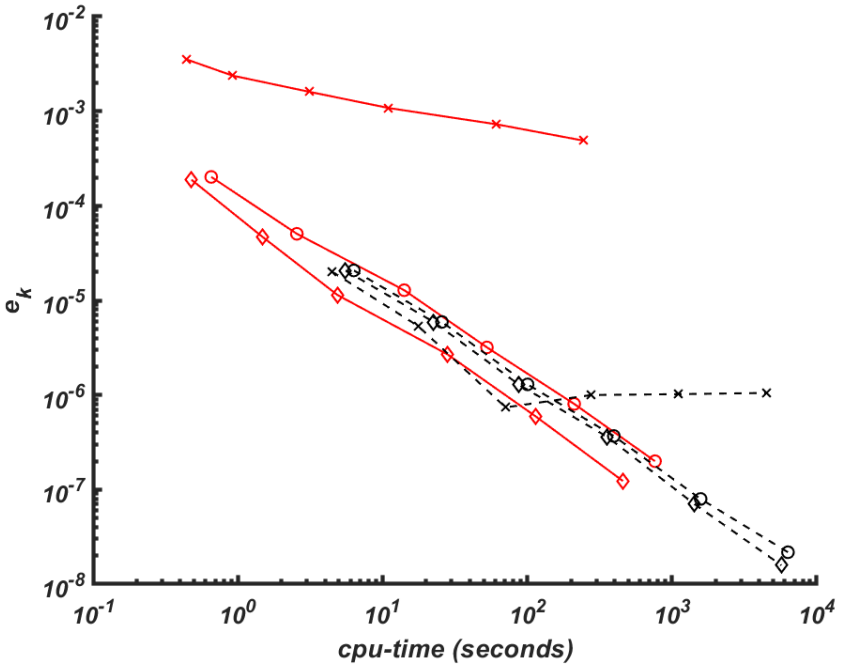

Figure 1: Efficiency plot (e_k vs. CPU time): comparison of the efficiency of new method and the method with truncated maximum age [8]. New method, (red) straight line with $K = 1$, $K_\beta = 0.35$ ($\diamond$); $K = 1$, $K_\beta = 0.7$ (x); $K = 1$, $K_\beta = 0.175$ (o). Method with truncated maximum age [8] (black) dashed line, $A_{\max} = 45$ ($\diamond$); $A_{\max} = 35$ (x); $A_{\max} = 50$ (o).

Calsina and Ripoll [11] provided an approximation to the limit cycle around its equilibrium by means of the linearization of (1.4)-(1.5) in a neighborhood of the equilibrium point, and state the estimation 3.9163 of the period of the cycle. A first numerical approximation to the nonlinear limit cycle was provided in [8], they employed a truncated model of the original (1.4)-(1.5), and provided an estimation of the period by means of interpolation with the value about 3.9857. In Figure 3, we show, in the phase plane of total populations (H, V), our approximation to the limit cycle for different values of the discretization parameters, the unstable steady state and the linear approximation to the stable limite cycle given in [11]. In detail, we employ a fixed value of K and K_β, to observe the convergence of the dynamics when the time discretization parameter, k, decreases to zero. In the figure, we represent the results we obtain with $k = 2.137 \cdot 10^{-2}$, by means of

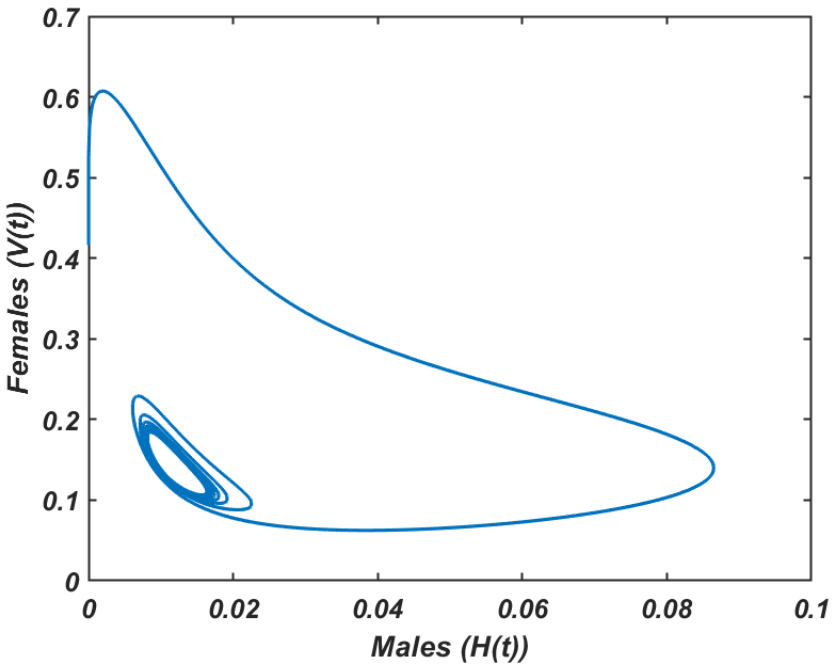

Figure 2: Evolution of the total populations in the unstable case.

a dashed line, $k = 1.0685 \cdot 10^{-2}$, with a dotted line, and $k = 5.3425 \cdot 10^{-3}$, in a solid line. Lower values of k match with the solid line. The same results are obtained with different values of the parameters K and K_β (not shown). Therefore, we can assure the convergence of the numerical solution to a limit cycle that we expect to be an approximation to the theoretical one (and quite different to the linear approximation). In this case, we can also fix the convergence of the period of such cycle to the value 3.985505, slightly different to the provided in the case of the truncated problem. Numerically, we have also discovered that the dynamics of the problem do not change any more until the extinction of both populations (not shown).

5. Conclusions

The main interest of modelling is to describe the behavior of the system we are interested in, through the analysis of the dynamics of the solutions of the mathematical model. In order to fit the dynamics of evolutionary problems, mathematical models could mix continuous and discrete features that

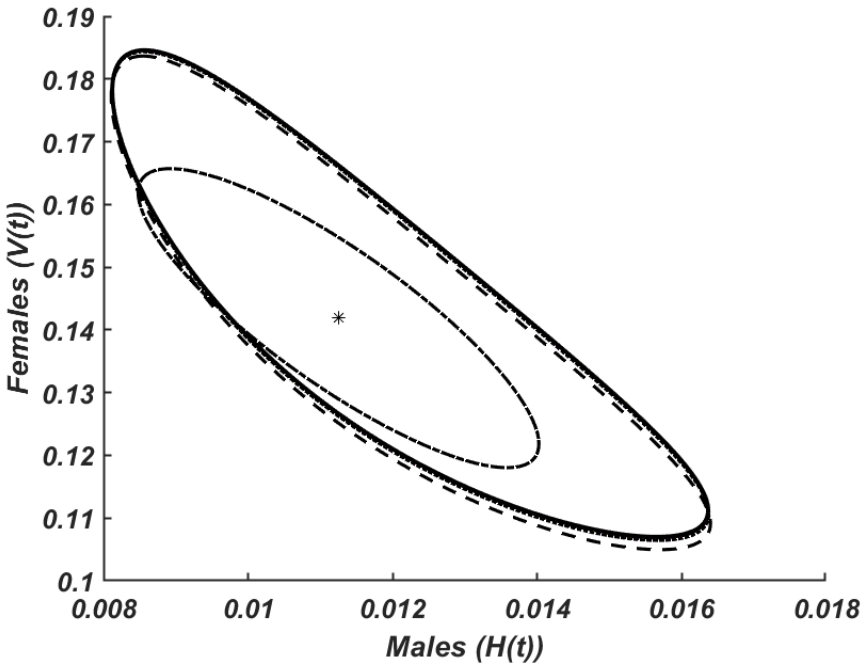

Figure 3: Unstable case. Equilibrium (*). Stable limit cycle approximation. $k = 2.137 \cdot 10^{-2}$ (dashed line), $k = 1.0685 \cdot 10^{-2}$ (dotted line), $k = 5.3425 \cdot 10^{-3}$ (solid line). Dot-dashed line corresponds to the stable limit cycle of the linearized problem [11].

complicate their analytical and numerical treatment. These features could be similar to the ones presented in the model we study: a compartmental age-structured population model with a sudden change in the balance law equations. Its analytical solution is not feasible and its asymptotic analysis is made by means of a linearization about the steady-state solution of the model equations. An alternative approach is to numerically approximate the asymptotic behavior of the solution through long-time integrations. In this case, the challenge is to verify that the discrete dynamics of the numerical method reports the continuous one faithfully.

We have employed a new numerical technique to solve age-structured models with an unbounded domain that was analyzed in [2]. It introduces a second order numerical discretization of a reformulation of the model problem in terms of a new computational size variable that evolves with age to cope with the difficulties of the infinite lifespan in long-time simulations.

This is employed to study the dynamics of a well-known model that describe the evolution of the sexual phase of *Monogonont rotifera*. The asymptotic behavior of this model was reported with classical analytical techniques in Calsina and Ripoll in [11]. They employed the male-female encounter rate parameter as a bifurcation parameter, and proved the existence of a Hopf bifurcation: a stable steady state that changes to unstable and the emergence of a stable limit cycle. The new proposal allows to study the problem numerically without the artificial truncation of the unbounded age interval as was done in [8]. We find good concordance between numerical predictions and the theoretical study. For the model problem we study, if the discretization parameters, K_β and K, of the new numerical method are properly chosen, then the new approach is more efficient, in terms of computational cost, than other numerical methods based on the discretization along the characteristics on a truncated domain. Parameter K_β should be chosen close to and below the exponential rate of decay of the solution of the problem to minimize the size of the natural grid of the discretization.

We study the dynamics of the numerical solution, and we discover the existence of a numerical steady state in the discrete dynamics. We prove the convergence of the numerical steady state to the theoretical one as the time discretization parameter decreases to zero. Also, we discover how the steady state loses its stability and a discrete limit cycle appears as the same bifurcation parameter (the male-female encounter rate) increases through a threshold value. We demonstrate numerically the convergence of this limit cycle to the theoretical one when the time discretization parameter goes to zero. Finally, we conclude that we provide an effective tool in the study of complex dynamics of age-structured models with infinite lifespan in which we can study the model without changing its complexity.

Acknowledgements

The authors were partially funded by project PID2020-113554GB-I00/AEI/10.13039/501100011033 of the Spanish Agencia Estatal de Investigación, Grant RED2022-134784-T by MCIN/AEI/10.13039/501100011033.

The authors are very grateful to the anonymous referees for their careful reading of the original manuscript and their contribution to its improving.

References

[1] Abia LM, Angulo O, López-Marcos JC. Age-structured population models and their numerical solution. Ecological Modelling 2005; 188:112-136.

[2] Abia LM, Angulo O, López-Marcos JC, López-Marcos MA. Numerical integration of an age-structured population model with infinite life span. Applied Mathematics and Computation 2022; 434:127401.

[3] Adimy M, Chekroun A, Dugourd-Camus C, Meghelli H. Global Asymptotic Stability of a Hybrid Differential–Difference System Describing SIR and SIS Epidemic Models with a Protection Phase and a Nonlinear Force of Infection. Qualitative Theory of Dynamical Systems 2024; 23:1-34.

[4] Adimy M, Crauste F, Ruan S. Modelling Hematopoiesis Mediated by Growth Factors With Applications to Periodic Hematological Diseases. Bulletin of Mathematical Biology 2006; 68:2321-2351.

[5] Angulo O, López-Marcos JC. Numerical schemes for size-structured population equations. Mathematical Biosciences 1999; 157:169-188.

[6] Angulo O, López-Marcos JC. Numerical integration of nonlinear size-structured population equations. Ecological Modelling 2000; 133:3-14.

[7] Angulo O, López-Marcos JC, Numerical integration of fully nonlinear size-structured population models. Appl. Numer. Math. 2004; 50:291-327.

[8] Angulo O, López-Marcos JC, López-Marcos MA. A numerical integrator for a model with a discontinuous sink term: the dynamics of the sexual phase of monogonont rotifera. Nonlinear Analysis RWA 2005; 6:935-954.

[9] Calsina A, Mazón JM, Serra M. A mathematical model for the phase of sexual reproduction in monogonont rotifers. J. Math. Biol. 2000; 40:451-471.

[10] J. M. Cushing. An Introduction to Structured Population Dynamics. CMB-NSF Regional Conference Series in Applied Mathematics **71**; Philadelphia: SIAM; 1998.

[11] Calsina A, Ripoll J. Hopf bifurcation in a structured population model for the sexual phase of monogonont rotifers. J. Math. Biol. 2002; 45:22-36.

[12] Cooke KL, van den Driessche P. Analysis of an SEIRS epidemic model with two delays. J. Math. Biol. 1996; 35:240-260.

[13] Iannelli M, Milner F. The Basic Approach to Age-Structured Population Dynamics. Dordrecht, The Netherlands: Springer; 2017.

[14] Martcheva M. An Introduction to Mathematical Epidemiology. Texts in Applied Mathematics 61. Springer; 2015.

[15] Perthame B. Transport Equations in Biology. Basel, Switzerland: Birkhäuser; 2007.

[16] Webb GF. Theory of Nonlinear Age-Dependent Population Dynamics. New York: Marcel Dekker; 1985.

[17] Zhao J, Lan R, Wang Z, Su W, Song D, Xue R, Liu Z, Liu X, Dai Y, Yue T, Xing B. Microplastic fragmentation by rotifers in aquatic ecosystems contributes to global nanoplastic pollution. Nature Nanotechnology 2024; 19:406-414.